BMC Plant Biology

RESEARCH Open Access

Biological activity of *Arabidopsis* flap endonuclease 1 (FEN1) is modulated by nuclear factors that inhibit its aggregation

Arkadiusz Borek[1], Piotr Bonarek[2], Ewa Kowalska[1], Agnieszka Katarzyna Banaś[1] and Wojciech Strzałka[1*]

Abstract

Flap endonuclease 1 (FEN1) is part of a group of nuclear enzymes involved in eukaryotic DNA replication and repair. In our studies, using both biochemical and biophysical approaches, we demonstrated that *Arabidopsis thaliana* FEN1 (AtFEN1) is unstable and prone to aggregation. To understand the reasons for AtFEN1 aggregation, we first analyzed the effects of heparin sodium and sodium chloride on its aggregation. We found that both heparin sodium and sodium chloride modulated the aggregation of this enzyme; however, achieving the same level of aggregation inhibition required using a sodium chloride concentration five orders of magnitude higher than that of heparin. Subsequently, to identify potential nuclear factors that may modulate the biological activity of AtFEN1 in vivo, we used DNA. Our experiments showed that negatively charged double-stranded DNA (dsDNA), similarly to the double-flap DNA (dfDNA) substrate of AtFEN1, inhibited AtFEN1 aggregation. This inhibitory effect was much less pronounced when single-stranded DNA (ssDNA) was used. Moreover, dfDNA prevented the loss of biological activity of AtFEN1. Finally, we revealed that AtFEN1 aggregation was also blocked by *Arabidopsis* proliferating cell nuclear antigen 1 (PCNA1), a natural interacting protein of AtFEN1. However, this effect was observed only when the putative PCNA-interacting protein (PIP)-box sequence was present in AtFEN1.

Highlights

- FEN1 is an unstable protein prone to aggregation.
- Ionic interactions modulate the stability of FEN1.
- Nuclear factors, including double-stranded DNA, help to modulate the biological activity of FEN1.

Keywords *Arabidopsis thaliana*, Cell proliferation, DNA replication and repair, Protein aggregation

*Correspondence:
Wojciech Strzałka
wojciech.strzalka@uj.edu.pl
[1]Department of Plant Biotechnology, Faculty of Biochemistry, Biophysics and Biotechnology, Jagiellonian University, Krakow, Poland
[2]Department of Physical Biochemistry, Faculty of Biochemistry, Biophysics and Biotechnology, Jagiellonian University, Krakow, Poland

Background

Flap endonuclease 1 (FEN1) is an enzyme that belongs to the Rad2 family of structure-specific nucleases [1]. It is primarily known for its essential role in DNA replication, including Okazaki fragment maturation (for a review, see Ma et al., 2022 [2]), resolution of trinucleotide repeat sequence-derived secondary structures [3], and rescue of stalled DNA replication forks [4]. Additionally, FEN1 is implicated in other major DNA metabolic pathways, including the maintenance of telomere stability, apoptotic fragmentation of DNA [5], homologous recombination [6], microhomology-mediated alternative end joining [7], and long-patch base excision repair [8]. The knockout of the gene encoding FEN1 is lethal in mammals and plants but not in yeast [9, 10]. Biochemical studies have revealed that human and yeast FEN1 enzymes exhibit three types of enzymatic activities: flap endonuclease (FEN), gap endonuclease (GEN), and exonuclease (EXO) [11, 12]. However, no exonuclease activity has been detected in *Arabidopsis* FEN1, indicating different protein properties compared to its human and yeast homologs [13]. FEN1 is composed of a nuclease core domain and a lysine-rich C-terminal tail. The C-terminus is involved in nonspecific DNA binding [14] and protein–protein interactions [15]. Predictions made by the AlphaFold algorithm indicate that, at least in the absence of a DNA substrate, the C-terminus of eukaryotic FEN1 remains unstructured. FEN1 interacts with proliferating cell nuclear antigen (PCNA) through its PCNA-interacting protein-box (PIP-box) motif. Studies of proteins from various organisms indicate that this motif is partly conserved among animal, yeast, and plant proteins interacting with PCNA. The canonical sequence of this motif follows the pattern: Q-x-x-(h)-x-x-(a)-(a), where "h" represents amino acids with moderately hydrophobic side chains (L, I, M), and "a" represents strongly hydrophobic residues with an aromatic side chain (Y, F) [16]. Binding with PCNA stimulates the FEN activity of the FEN1 enzyme. Mutational analyses have shown that the formation of FEN1/PCNA complexes and the effectiveness of PCNA-dependent stimulation of FEN1 activity depend on the presence of a correctly structured PIP-box sequence in the FEN1 protein [17]. Among the functional units involved in DNA replication and repair is the FEN1/PCNA/DNA complex. Biophysical studies have revealed that upon FEN1 binding, the DNA substrate bends [18]. To better understand the details of the reaction performed by FEN1, the three-dimensional structures of human FEN1/PCNA [19] and FEN1/DNA substrate complexes [20] have been determined. Moreover, high-resolution structure of the complex of DNA with two human proteins, FEN1 and PCNA has been obtained [21].

The regulation of the activity and stability of proteins involved in DNA replication and repair, including FEN1, is crucial for proper cellular function. This regulation involves various processes, such as protein folding, interactions with other proteins (e.g., the FEN1/PCNA complex), and posttranslational modifications. While studying AtFEN1, we found that this protein is unstable and prone to aggregation. Although aggregation can be a physiological process, it may also involve misfolded or unstable proteins, potentially disrupting their function. Using turbidity and fluorescence polarization assays, we demonstrated a relationship between AtFEN1 aggregation and its biological activity.

Materials and methods

Proteins, oligonucleotides, and DNA Preparation

Cytochrome *c* was purchased from Sigma-Aldrich. The following oligonucleotides were purchased from Eurofins (Austria) and dissolved in sterile water (concentration 100 μM): ssDNA (5′-TTTTTTTTTTTTTTTCCCCCCCCCCCCCCC-3′), ssDNAcomp (5′-GGGGGGGGGGGGGGGAAAAAAAAAAAAAAA-3′), D (5′-ACTCTGCCTCAAGACGGTTCAGTCCGACAT-3′), U (5′-ATGAGGCAGAGT-3′), UF (5′-ATGTCGGACTGAACCGTCC-3′), A (5′-GATGACGAGCAGTCCTAACTGGAAATCTAGCTCTGTCAACACCAACAGAGCTAGATTTCCC-3′), and B (5′-Phospho T[Atto495]TTTTTTTTTAGTTAGGACTGCTCGTCATC-3′) dsDNA was prepared by annealing the ssDNA and ssDNAcomp oligonucleotides. The double-flap DNA (dfDNA) substrate was assembled by annealing the U, D, and UF oligonucleotides. The Atto495 dfDNA substrate used for FEN activity analysis was prepared by annealing the A and B oligonucleotides. A 10 μM solution of ssDNA, dsDNA, or DNA substrates, prepared in annealing buffer (20 mM Tris-HCl, pH 7.8, supplemented with 25 mM NaCl), was heated to 95 °C for 3 min and then cooled to 20 °C at a rate of 1 °C/min using T100 thermal cycler (Bio-Rad, Singapore).

Cloning and vectors

The open reading frame (ORF) of *Arabidopsis* FEN1 (NCBI accession number NM_001161268) was amplified using Phusion High-Fidelity DNA Polymerase (Thermo Fisher Scientific, Lithuania) with the primers AtFEN-1FWG (5′-GGGGACAAGTTTGTACAAAAAAGCAGGCTCCATGGGTATTAAGGGTTTAACGAAGC-3′) and AtFEN1RWG (5′-GGGGACCACTTTGTACAAGAAAGCTGGGTCCTTCTTCTTCCTTCCACCAGCTCC-3′), along with *Arabidopsis* cDNA. Following an initial denaturation step at 95 °C for 5 min, 30 cycles of amplification were performed, consisting of denaturation at 95 °C for 30 s, annealing at 50 °C for 30 s, and DNA synthesis at 72 °C for 2 min, followed by a final incubation at 72 °C for 5 min in a T100 thermal cycler (Bio-Rad, Singapore). The resulting PCR product was purified and cloned into the pDONR221 vector using a Gateway BP

reaction (Thermo Fisher Scientific), followed by sequencing. The pDONR221 vector carrying the cDNA sequence encoding the AtFEN1 PIP-box mutant was purchased from GenScript. The ORFs of AtFEN1 and AtFEN1 PIP-box were transferred into the expression vector pDEST17 using a Gateway LR reaction (Life Technologies). The construction of the pET15bAtPCNA1 vector was previously described [22].

Protein production and purification

Expression vectors encoding the appropriate ORFs were transformed into *Escherichia coli* BL21 (DE3) CodonPlus-pRIL strain cells for recombinant protein production. The bacteria were grown at 37 °C in LB medium supplemented with ampicillin (100 mg/L) and chloramphenicol (25 mg/L). When the optical density of the bacterial culture at 600 nm (OD_{600}) reached 0.6, protein production was induced using 1 mM IPTG for AtPCNA1 or 0.3 mM IPTG for AtFEN1 and AtFEN1 PIP-box. The bacteria were then grown with vigorous shaking at 37 °C for 4 h (AtPCNA1) or at 14 °C for 16 h (AtFEN1 and AtFEN1 PIP-box). Next, the cells were harvested by centrifugation (5 min, 8,000×g, 4 °C). AtPCNA1 was purified following a previously described protocol [22, 23]. Bacterial cells producing AtFEN1 or AtFEN1 PIP-box were resuspended in buffer A (50 mM MOPS, 1 M NaCl, 20 mM imidazole, pH 7.5). The cells were lysed by sonication for 7 min (5-s pulses with 15-s pauses) using an Omni-Ruptor 4000 sonicator (OMNI International Inc., USA). The lysate was centrifuged (20 min, 30,000×g, 4 °C), and the soluble protein extract was loaded onto Ni-NTA Sepharose (GE Healthcare, Sweden). The protein was washed with buffer A and eluted in buffer B (50 mM MOPS, 1 M NaCl, 300 mM imidazole, pH 7.5). After elution, the protein was dialyzed into buffer C (50 mM MOPS, 1 M NaCl, pH 7.5), frozen in liquid nitrogen, and stored at – 80 °C until use.

Turbidity assay

Protein turbidity was measured using a Shimadzu UV-2101PC (Japan) spectrophotometer by recording the absorption at 400 nm (or 500 nm when cytochrome *c* was used) of the reaction mixture, which was stirred in a Hellma Semi-Micro Cuvette 119.004-QS. Turbidity rates (aggregation rates) were calculated from the initial linear portions of the kinetic traces based on time-dependent absorption recorded at 400–500 nm. The reaction mixture had a total volume of 0.75 mL and consisted of 50 mM MOPS (pH 7.5) supplemented with NaCl (ranging from 0.01 to 1 M). For each sample, 3–5 measurements were recorded. The concentrations of AtFEN1, other proteins, and substances in the reaction mixture were as described in the figure legends.

Protein unfolding assays

Thermal stability, monitored by differential scanning fluorimetry (DSF), was performed using a Prometheus NT.48 (NanoTemper Technologies, Germany) with a sample volume of approximately 10 µL per capillary. Thermal stability, monitored by the circular dichroism (CD) signal at 220 nm, was measured using a JASCO J-710 (Japan) spectropolarimeter with a 1 mm pathlength quartz cuvette and a sample volume of approximately 350 µL. Measurements were conducted at a protein concentration of 10 µM in 50 mM sodium phosphate buffer, pH 7.5, supplemented with 100, 300, or 1,000 mM NaF. Scans were performed in triplicate over a temperature range of 15–80 °C, with a heating rate of 1 °C/min. Thermal transition temperatures (T_m) were defined as the mean of the maximum values of the first derivative of the signals in the transition region.

AtFEN1 activity assay based on fluorescence polarization

The FEN activity of AtFEN1 was analyzed with the help of Tecan Infinite 200 PRO (Austria) spectrophotometer using a fluorescence polarization (FP) DNA cleavage assay [24] with minor modifications. The total reaction volume was 20 µL and consisted of 30 nM AtFEN1 and 30 nM Atto495 dfDNA substrate dissolved in activity buffer (20 mM Tris-HCl, pH 7.4, 10 mM KCl, 10 mM $MgCl_2$, 0.01% (v/v) Tween 20, 5% (v/v) glycerol, 0.1 mg/mL BSA, and 1 mM DTT). The enzymatic reaction was performed at 25 °C. Changes in the FP signal were measured for AtFEN1 samples preincubated with or without the DNA substrate over 378 min. For each sample, 3–5 measurements were recorded. The background activity, determined by monitoring fluorescence polarization changes in the Atto495 dfDNA substrate over 378 min, was negligible (Supplementary Fig. 1, Supplementary Table 1).

Results

Aggregation of *Arabidopsis* FEN1 is modulated by electrostatic interactions

Our results show that in the presence of 300 mM NaCl, AtFEN1 (10 µM) was prone to aggregation. Reducing the NaCl concentration from 300 to 10 mM led to significant precipitation of AtFEN1, indicating a strong correlation between AtFEN1 aggregation and electrostatic interactions. This relationship was further confirmed by assessing AtFEN1 aggregation at varying NaCl concentrations. While AtFEN1 aggregated rapidly in the presence of 10 mM NaCl (Fig. 1A), the aggregation rate decreased as the NaCl concentration increased. In the range of 0.6 to 1 M NaCl, AtFEN1 aggregation was practically undetectable. A similar effect was observed when NaF was used instead of NaCl (Supplementary Fig. 2). Since manipulation of the ionic strength of the buffer allowed for easy

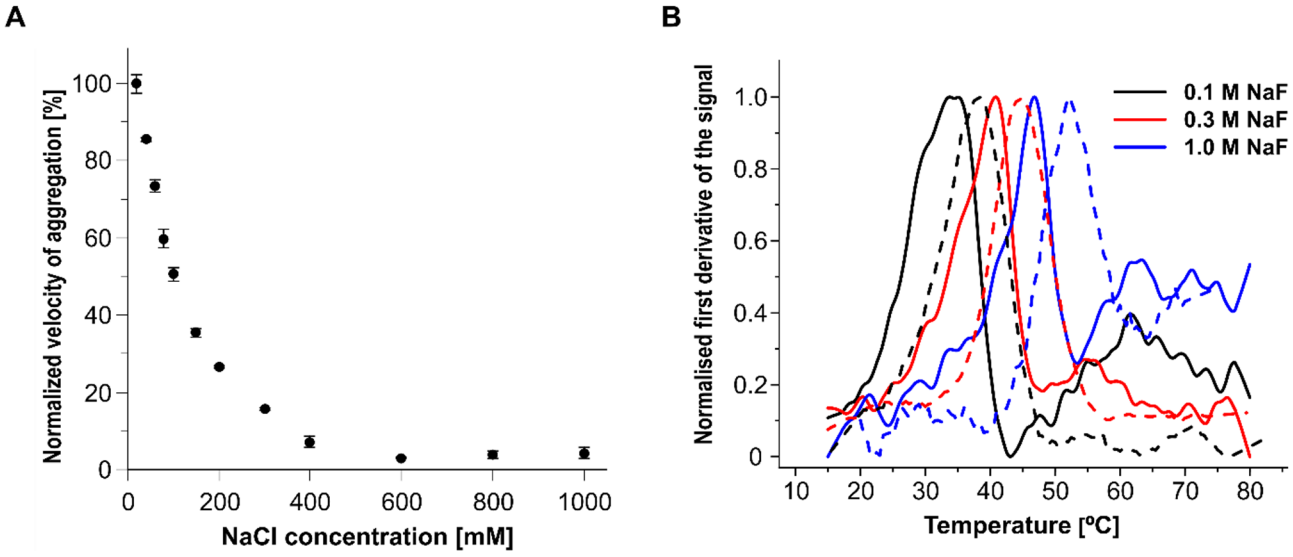

Fig. 1 Effect of buffer ionic strength on the aggregation and thermal stability of AtFEN1. (**A**) Aggregation of 4 µM AtFEN1 in the presence of increasing NaCl concentrations (0.01 to 1 M) at room temperature, monitored by a turbidity assay at 400 nm. The results represent the mean of three independent experiments, with error bars indicating standard deviation. (**B**) Dependence of AtFEN1 thermal stability on buffer ionic strength, measured using differential scanning fluorimetry (DSF) (solid lines) and circular dichroism (**CD**) spectroscopy (dashed lines). A 10 µM protein sample dissolved in buffer was supplemented with 0.1 M (black), 0.3 M (red), or 1 M (blue) NaF. Thermal denaturation profiles were recorded at 330 and 350 nm for DSF and at 220 nm for CD. The figure presents representative data from one of three independent experiments, with averaged profiles shown

Table 1 Thermal transition temperatures (T_m) of AtFEN1 in solutions with different concentrations of NaF, measured by CD and DSF methods (Fig. 1). Measurement errors were below ± 1 °C

[NaF] (M)	CD	nanoDFS
0.1	39 °C	34 °C
0.3	45 °C	40 °C
1	52 °C	47 °C

modulation of AtFEN1 aggregation at room temperature, we next used CD spectroscopy and DSF to analyze the thermal stability of AtFEN1 at three different NaF concentrations (Fig. 1B). In these experiments, NaF was chosen over NaCl because chloride ions in aqueous solutions exhibit high absorbance below 200 nm. The thermal transition temperature (*Tm*) values obtained are summarized in Table 1. The systematic difference between the *Tm* values determined by the two methods indicates the presence of intermediate states of AtFEN1. Regardless of the method used, the lowest phase transition temperature was observed for AtFEN1 in buffer supplemented with 0.1 M NaF, while in the presence of 1 M NaF, this temperature increased by approximately 13 °C.

In the next step, we aimed to evaluate the effect of heparin, which can bind many proteins, including those that bind DNA, as it mimics the polyanionic structure of nucleic acids. For this purpose, we used sodium heparin. We found that AtFEN1 (5 µM) aggregation was completely inhibited in the presence of sodium heparin at concentrations equal to or greater than 4 µM (i.e., above 0.04 mg/mL) (Fig. 2A). To determine whether, similar to our observations with ions, heparin inhibition of AtFEN1 aggregation also increased the thermal stability of this protein, we used the DSF technique. We confirmed the positive effect of sodium heparin on the thermal stability of AtFEN1. While the phase transition temperature of AtFEN1 in buffer containing 0.1 M NaF (control) was approximately 35 °C, it increased to 46 °C following the addition of heparin (10 µM, 0.1 mg/mL) (Fig. 2B).

DNA and PCNA modulate biological activity of *Arabidopsis* FEN1

To date, our in vitro studies have shown that AtFEN1 is an unstable protein prone to aggregation in a low-ionic-strength buffer (Fig. 1). Moreover, this process can be modulated by molecules carrying negative charges (Fig. 2A). Based on this information, we hypothesized that such molecules present in the cell nucleus may function as natural antiaggregation factors for AtFEN1. On this basis, we proposed that DNA and PCNA could act as natural modulators of AtFEN1's biological activity. To test this hypothesis, we first analyzed AtFEN1 aggregation in the presence of 20 mM NaCl and different DNA molecules, including single-stranded DNA (ssDNA), double-stranded DNA (dsDNA), and double-flap (df) DNA, the substrate of AtFEN1 (Fig. 3A). While dsDNA and dfDNA effectively blocked AtFEN1 aggregation, ssDNA was largely ineffective.

The aim of our next experiment was to determine whether the enzymatic activity of AtFEN1 depends on its aggregation. For this purpose, AtFEN1 was placed in

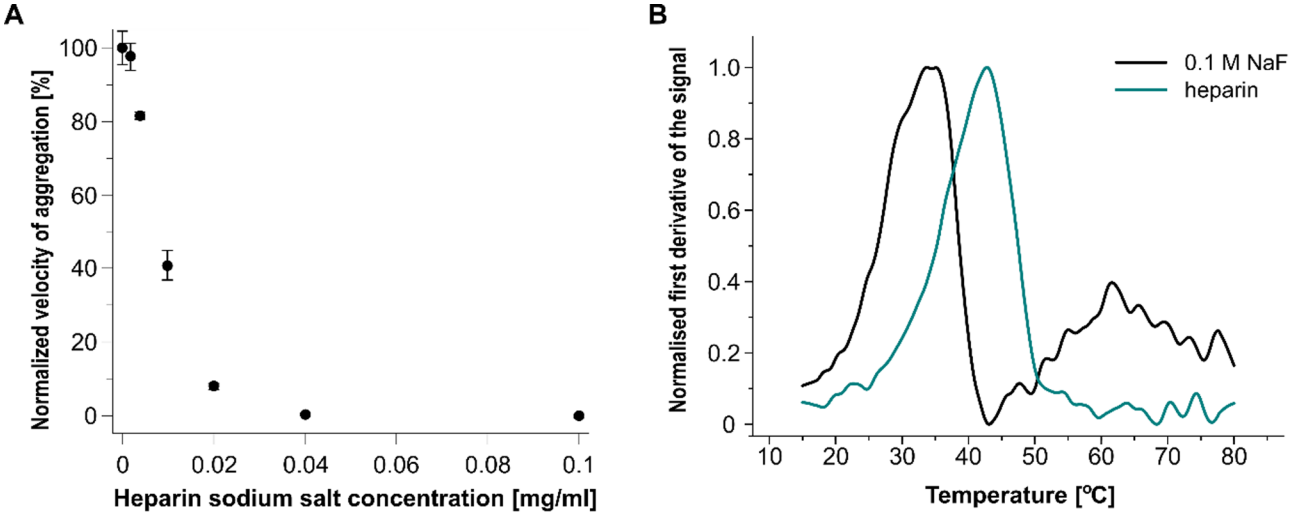

Fig. 2 Impact of heparin sodium salt on the aggregation and thermal stability of AtFEN1. (**A**) Aggregation of 4 µM AtFEN1 in the presence of increasing concentrations of heparin sodium salt (0 to 0.1 mg/mL), monitored using a turbidity assay at 400 nm. The results represent the mean of three independent experiments, with error bars indicating standard deviation. (**B**) Effect of heparin sodium salt on the thermal stability of AtFEN1, measured using DSF. A 10 µM protein sample, either without (black) or with (green) 0.1 mg/mL heparin sodium salt, was heated from 20 °C to 55 °C. The thermal denaturation profile was recorded at 330 and 350 nm. Averaged profiles are shown. The figure presents representative data from one of three independent experiments

a low-ionic-strength buffer (10 mM KCl) lacking divalent ions required for its activity. Two sets of samples were then prepared (Supplementary Fig. 3). The first set contained dfDNA labeled with the fluorescent dye Atto495. dfDNA serves as a substrate for AtFEN1 and, according to our results, inhibits AtFEN1 aggregation. In these samples, the enzymatic reaction was initiated by the addition of magnesium chloride. In the second set, after preincubating AtFEN1 with magnesium chloride, the enzymatic reaction was triggered by the addition of the substrate, Atto495 dfDNA. The presence of Atto495 dfDNA during preincubation had a significant effect on the enzymatic activity of AtFEN1 (Fig. 3B). While activity remained constant throughout the preincubation period with Atto495 dfDNA, a steady decrease was observed in samples preincubated with magnesium chloride. After 378 min of preincubation without the substrate, AtFEN1 activity was only 20% of that observed in samples preincubated with Atto495 dfDNA.

Lastly, we evaluated whether *Arabidopsis* PCNA1 protein could modulate AtFEN1 aggregation. AtPCNA1:AtFEN1 molar ratios of 1.5 or greater effectively prevented AtFEN1 aggregation (Fig. 3C). The interaction between PCNA and FEN1 is mediated by the PCNA-interacting protein (PIP)-box sequence present in FEN1 [17]. We therefore investigated whether the presence of the putative PIP-box in AtFEN1 affects its aggregation inhibition by PCNA. To do this, we produced and purified version of AtFEN1 in which selected amino acid residues (Supplementary Fig. 4) of the putative PIP-box sequence were mutated to alanine. These mutant should have an impaired interaction with PCNA [17]. We found that, under the conditions tested, AtPCNA1 effectively inhibited the aggregation of wild-type AtFEN1 but not the AtFEN1 PIP-box mutant. The AtFEN1 mutant with the impaired PIP-box sequence remained prone to aggregation even at the highest concentration of AtPCNA1 (i.e., an AtPCNA1:AtFEN1 equal to 3 molar ratio). To rule out the possibility that AtPCNA1-dependent inhibition of AtFEN1 aggregation was simply a crowding effect, we tested whether the addition of bovine cytochrome *c* influenced AtFEN1 aggregation (Fig. 3D). We observed slightly reduced aggregation of AtFEN1 in the presence of high concentrations of cytochrome *c* (10 µM). This effect may be due, in part, to the dipolar nature of cytochrome *c*, which, at the low ionic strength used in the experiment, can nonspecifically bind to both positively and negatively charged regions of AtFEN1. Our results clearly show that the inhibition of AtFEN1 aggregation is specifically associated with its interaction with AtPCNA1.

Discussion

FEN1 is a protein of fundamental importance for higher eukaryotes, including plants [13]. A significant number of studies have focused on human and yeast FEN1, addressing, among other topics, its role in DNA replication and the repair of DNA lesions [5]. Despite the growing body of data on FEN1, the factors that can modulate its aggregation, thermal stability, and, consequently, its biological activity have yet to be thoroughly investigated or discussed. Therefore, the aim of our study was to fill this gap. For our model protein, we used *Arabidopsis* FEN1.

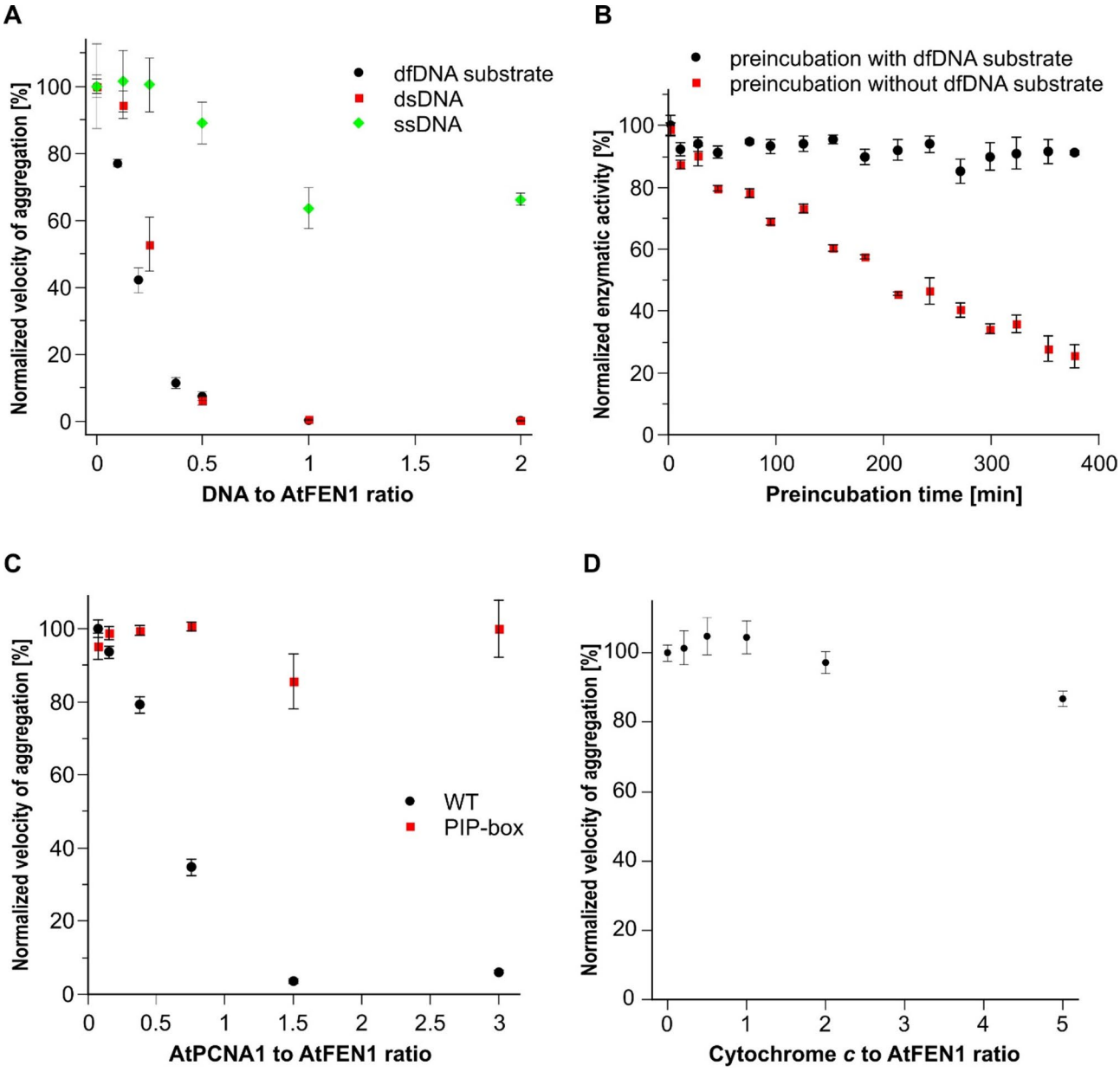

Fig. 3 Impact of DNA and PCNA on the aggregation of AtFEN1. (**A**) Aggregation of 4 µM AtFEN1 was analyzed in the presence of increasing concentrations of DNA (0 to 8 µM, DNA/AtFEN1 ratio from 0 to 2) and monitored using a turbidity assay at 400 nm. Black dots, red squares, and green diamonds represent the AtFEN1 substrate (dfDNA), dsDNA, ssDNA, respectively. (**B**) Influence of preincubation of Atto495 dfDNA substrate with AtFEN1 on the enzymatic activity of the protein. AtFEN1 activity was measured as changes in fluorescence polarization of the Atto495 dfDNA substrate in samples preincubated with or without the Atto495 dfDNA substrate for 378 min. Black dots and red rectangles represent AtFEN1 samples preincubated with or without the Atto495 dfDNA substrate, respectively. (**C**) Influence of at PCNA1 on the aggregation of at FEN1 and the AtFEN1 PIP-box mutant. Aggregation of 2 µM AtFEN1/AtFEN1 PIP-box mutant was analyzed in the presence of increasing concentrations of AtPCNA1 (0 to 6 µM) and monitored using a turbidity assay at 400 nm. Black dots and red rectangles represent AtFEN1 and the AtFEN1 PIP-box mutant, respectively. (**D**) Impact of cytochrome *c* on the aggregation of AtFEN1. Since cytochrome *c* absorbs light at 400 nm, detection was performed at 500 nm, where cytochrome *c* does not absorb light. The results represent the mean of three independent experiments, with error bars indicating standard deviation

Ionic interactions modulate the aggregation of AtFEN1

The results of our experiments indicate that the aggregation of AtFEN1 is caused by electrostatic interactions between its molecules. Ionic interactions between the positively charged fragments (e.g., the C-terminal tail and a fragment of its active site, Fig. 4) and negatively charged fragments (marked in red in Fig. 4) of AtFEN1, which occur under low ionic strength conditions, result in the aggregation of this protein (Fig. 5A). The more than 100,000-fold difference between the effective concentrations of NaCl (600 mM) and sodium heparin (4 µM) that inhibit AtFEN1 aggregation to a similar extent is likely

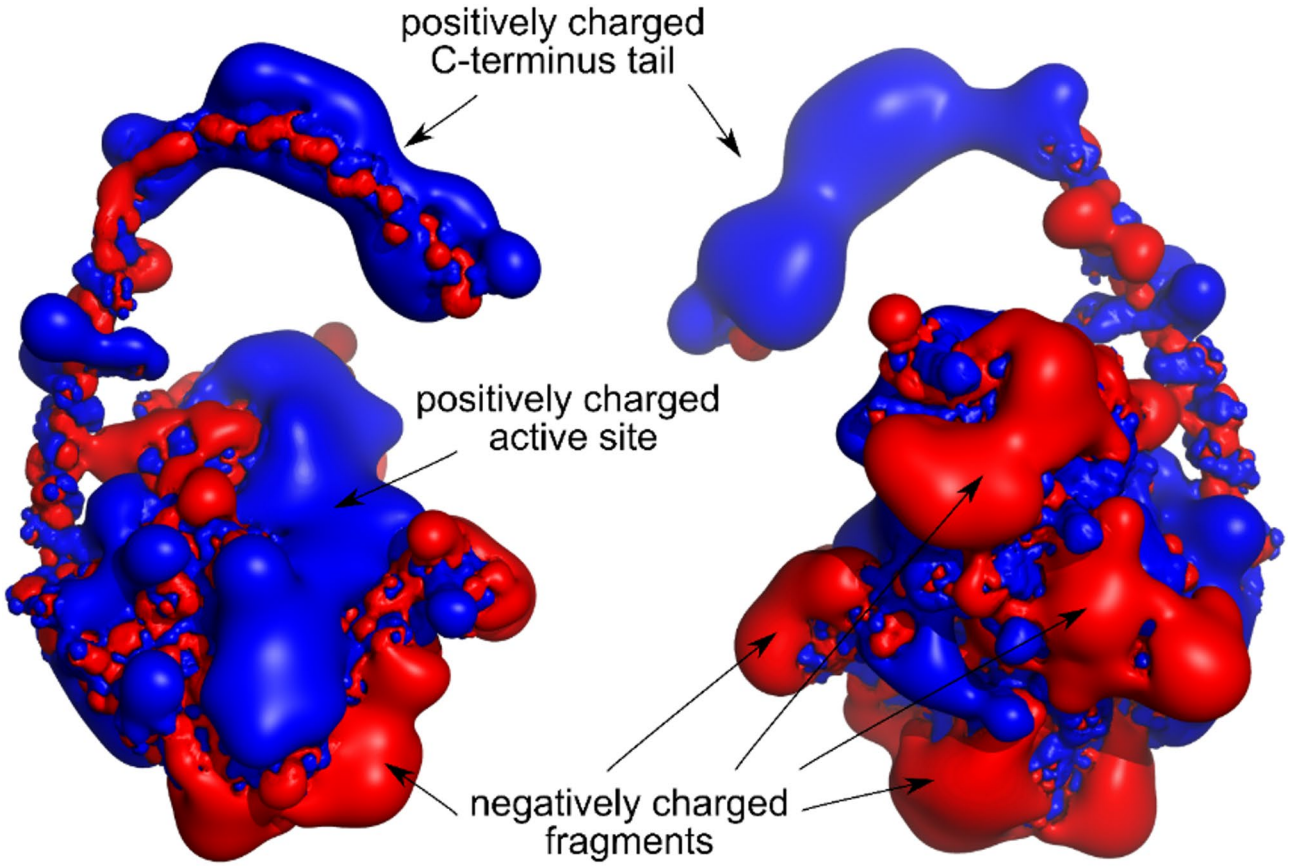

Fig. 4 Visualization of the surface charge distribution of AtFEN1, generated using the APBS tools 2.1 plugin for PyMOL [29]. The structure of AtFEN1 was predicted using AlphaFold. Positively charged fragments are shown in blue, while negatively charged fragments are shown in red. The molecule on the right side of the figure represents the same structure as on the left, rotated by 180°

due to differences in the molecular structures of these compounds. Heparin is a highly anionic polysaccharide, consisting of a mixture of linear chains made up of varying numbers of repeating disaccharide units, which include negatively charged sulfonated glucosamine and iduronic acid [25]. The polyanionic properties of heparin have previously been employed in chromatography for the purification of DNA-binding proteins, including FEN1 [20].

The average molecular weight of this polyanionic structure, which mimics nucleic acids such as DNA was 10 kDa. Therefore, the sodium heparin molecule contains significantly more negatively charged groups (on average, about 50 negatively charged groups per heparin molecule) and accompanying positively charged sodium ions than the NaCl molecule. Hence, the concentration of these negative residues in 4 μM heparin is approximately three orders of magnitude lower than the concentration of chloride anions in 1 M NaCl. The fact that five orders of magnitude fewer heparin molecules are required than NaCl to effectively protect AtFEN1 from aggregation indicates that the role of heparin extends beyond simply electrostatically screening interactions between AtFEN1 molecules; electrostatic interactions between heparin and AtFEN1 also play a role.

Electrostatic interactions not only modulate the aggregation degree of the AtFEN1 protein but also influence its thermal stability. Similar *Tm* values are observed with the addition of 1 M NaF or 10 μM heparin. The increased thermal stability of AtFEN1 is therefore not solely due to the rise in ionic strength but is likely also affected by a shift in the equilibrium between two conformations of AtFEN1 in its native state—one with lower thermal stability and a greater tendency to aggregate, and the other with higher thermal stability but a reduced tendency to aggregate (Figs. 1 and 2). By increasing the salt concentration or adding heparin, the equilibrium is shifted towards the more stable conformation of AtFEN1, resulting in reduced aggregation and an increase in its *Tm*.

Potential nuclear modulators of AtFEN1 biological activity

The observed in vitro aggregation of AtFEN1 under conditions of low ionic strength led us to question whether any molecules present in the cell nucleus could affect this process. Given that FEN1 is a structurally specific nuclease [26], we examined how the presence of ssDNA,

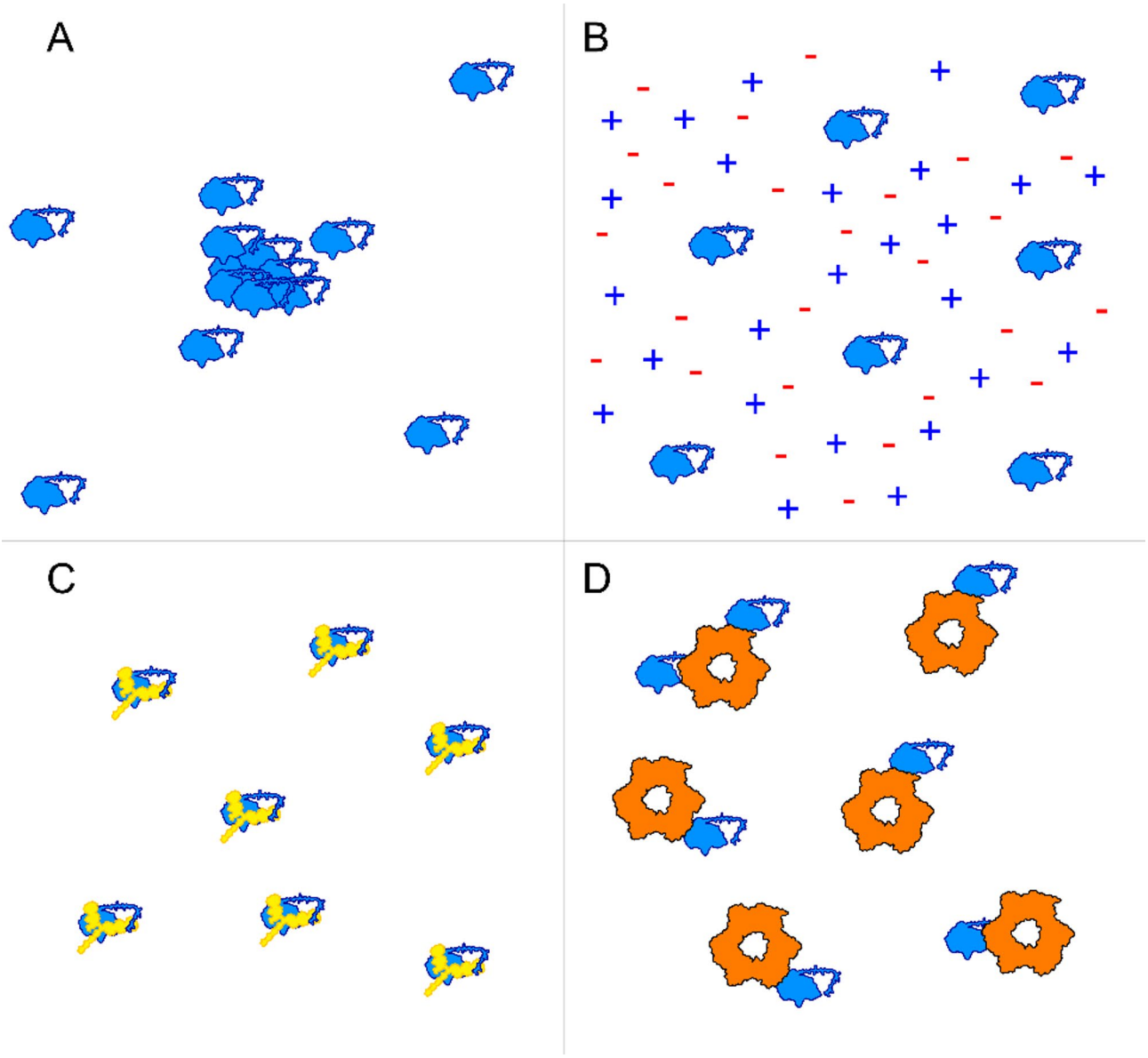

Fig. 5 Schematic summary of conditions affecting AtFEN1 aggregation. (**A**) At low ionic strength, AtFEN1 exhibits a tendency to aggregate. (**B**) A high NaCl concentration inhibits aggregation of this endonuclease by shielding electrostatic interactions between protein molecules. (**C**) Binding of dsDNA (yellow) to AtFEN1 masks the strong positive charge of the protein's active site, preventing aggregation. (**D**) Binding of AtFEN1 molecules to the AtPCNA1 ring (orange) prevents aggregation of the enzyme

dsDNA, and substrate dfDNA influences AtFEN1 aggregation (Fig. 3A). The binding of ssDNA and dsDNA to human FEN1 has been previously confirmed [27, 28]. Our results showed that only dsDNA and dfDNA, but not ssDNA, effectively blocked AtFEN1 aggregation. This is consistent with previous reports indicating that FEN1 binds ssDNA much more weakly than dsDNA and dfDNA [27, 28]. In the buffer containing KCl, the affinity of FEN1 for the tested DNA was observed in the following order: FEN1-ssDNA < FEN1-dsDNA < FEN1-dfDNA. This suggests that the lower total negative charge of ssDNA compared to dsDNA accounts for both its weaker affinity for FEN1 and its less effective inhibition of AtFEN1 aggregation. It cannot be excluded that the differences in the efficiency of ssDNA and dsDNA inhibition may also result from differences in their three-dimensional structures.

The observed in vitro inhibition of AtFEN1 aggregation by AtPCNA1, dsDNA, and the substrate dfDNA (Fig. 3) suggests that similar roles may be played in vivo by selected proteins present in the cell nucleus as well as DNA itself. The lack of changes in the activity of AtFEN1 preincubated with the substrate dfDNA at room temperature (Fig. 3B), along with the dependence of AtFEN1

aggregation on the presence of the putative PIP-box motif that ensures interaction with PCNA, although not providing final confirmation, supports this hypothesis. Regardless of the mechanisms preventing intramolecular interactions of AtFEN1, their effect is the inhibition of aggregation of this protein.

Conclusion

Our results clearly show that *Arabidopsis* FEN1 is an unstable protein prone to aggregation. Similar properties have been observed for human and yeast FEN1 (unpublished data). Our results indicate that molecules present in the cell nucleus, such as DNA and proteins interacting with FEN1, can modulate its aggregation and biological activity. However, the question remains: Is AtFEN1 unstable in the plant cell nucleus? The answer to this question will only be achievable once new techniques are developed to verify in vivo the experimental data obtained in vitro.

Abbreviations

At	Arabidopsis thaliana
dfDNA	Double-flap DNA
dsDNA	Double-stranded DNA
ssDNA	Single-stranded DNA
FEN1	Flap endonuclease 1
ORF	Open reading frame
PCNA	Proliferating cel nucelar antigen
PIP box	PCNA interacting protein box

Supplementary Information

The online version contains supplementary material available at https://doi.org/10.1186/s12870-025-06671-y.

Supplementary Material 1

Acknowledgements

We would like to thank Mr. Piotr Źrebiec for his technical support during the experiments. The open-access publication has been supported by theFaculty of Biochemistry, Biophysics and Biotechnology under the StrategicProgramme Excellence Initiative at Jagiellonian University in Krakow, Poland.

Author contributions

Conceptualization, A.B., W.S.; investigation, A.B., P.B., E.K., A.K.B; writing original draft, W.S. A.B., P.B.; writing, review and editing, W.S., A.B., E.K. and A.K.B., project administration, W.S.; funding acquisition, W.S.

Funding

This project was supported by the National Science Center, Poland, under grant UMO-2019/33/B/NZ3/01568 to W.S.

Data availability

Data supporting the results reported in the article are available from the corresponding author upon request.

Declarations

Ethics approval and consent to participate

Not applicable.

Consent for publication

Not applicable.

Competing interests

The authors declare no competing interests.

Received: 3 January 2025 / Accepted: 5 May 2025
Published online: 16 May 2025

References

1. Harrington JJ, Lieber MR. Functional domains within FEN-1 and RAD2 define a family of structure-specific endonucleases: implications for nucleotide excision repair. Genes Dev. 1994;8:1344–55. https://doi.org/10.1101/gad.8.11.1344.
2. Ma L, Sun H, Abeywardana T, Zheng L, Shen B. Structure-specific nucleases: role in Okazaki fragment maturation. Trends Genet. 2022;38:793–6. https://doi.org/10.1016/j.tig.2022.04.001.
3. Spiro C, Pelletier R, Rolfsmeier ML, Dixon MJ, Lahue RS, Gupta G, et al. Inhibition of FEN-1 processing by DNA secondary structure at trinucleotide repeats. Mol Cell. 1999;4:1079–85. https://doi.org/10.1016/S1097-2765(00)80236-1.
4. Zheng L, Zhou M, Chai Q, Parrish J, Xue D, Patrick SM, et al. Novel function of the flap endonuclease 1 complex in processing stalled DNA replication forks. EMBO Rep. 2005;6:83–9. https://doi.org/10.1038/sj.embor.7400313.
5. Zheng L, Jia J, Finger LD, Guo Z, Zer C, Shen B. Functional regulation of FEN1 nuclease and its link to cancer. Nucleic Acids Res. 2011;39:781–94. https://doi.org/10.1093/nar/gkq884.
6. Kikuchi K, Taniguchi Y, Hatanaka A, Sonoda E, Hochegger H, Adachi N, et al. Fen-1 facilitates homologous recombination by removing divergent sequences at DNA break ends. Mol Cell Biol. 2005;25:6948–55. https://doi.org/10.1128/mcb.25.16.6948-6955.2005.
7. Sharma S, Javadekar SM, Pandey M, Srivastava M, Kumari R, Raghavan SC. Homology and enzymatic requirements of microhomology-dependent alternative end joining. Cell Death Dis. 2015;6:e1697. https://doi.org/10.1038/CDDIS.2015.58.
8. Asagoshi K, Tano K, Chastain PD, Adachi N, Sonoda E, Kikuchi K, et al. FEN1 functions in long patch base excision repair under conditions of oxidative stress in vertebrate cells. Mol Cancer Res. 2010;8:204–15. https://doi.org/10.1158/1541-7786.MCR-09-0253.
9. Kucherlapati M, Yang K, Kuraguchi M, Zhao J, Lia M, Heyer J, et al. Haploinsufficiency of flap endonuclease (Fen1) leads to rapid tumor progression. Proc Natl Acad Sci U S A. 2002;99:9924–9. https://doi.org/10.1073/pnas.152321699.
10. Zhang J, Xie S, Zhu J-K, Gong Z. Requirement for flap endonuclease 1 (FEN1) to maintain genomic stability and transcriptional gene Silencing in Arabidopsis. Plant J. 2016;629–40. https://doi.org/10.1111/tpj.13224.
11. Sun H, He L, Wu H, Pan F, Wu X, Zhao J, et al. The FEN1 L209P mutation interferes with long-patch base excision repair and induces cellular transformation. Oncogene. 2017;36:194–207. https://doi.org/10.1038/onc.2016.188.
12. Singh P, Zheng L, Chavez V, Qiu J, Shen B. Concerted action of exonuclease and gap-dependent endonuclease activities of FEN-1 contributes to the resolution of triplet repeat sequences (CTG) n- and (GAA)n-derived secondary structures formed during maturation of Okazaki fragments. J Biol Chem. 2007;282:3465–77. https://doi.org/10.1074/jbc.M606582200.
13. Zhang Y, Wen C, Liu S, Zheng L, Shen B, Tao Y. Shade avoidance 6 encodes an arabidopsis flap endonuclease required for maintenance of genome integrity and development. Nucleic Acids Res. 2016;44:1271–84. https://doi.org/10.1093/nar/gkv1474.
14. Stucki M, Jónsson ZO, Hübscher U. In eukaryotic flap endonuclease 1, the C terminus is essential for substrate binding. J Biol Chem. 2001;276:7843–9. https://doi.org/10.1074/jbc.M008829200.
15. Guo Z, Chavez V, Singh P, Finger LD, Hang H, Hegde ML, et al. Comprehensive mapping of the C-terminus of flap endonuclease-1 reveals distinct interaction sites for five proteins that represent different DNA replication and repair pathways. J Mol Biol. 2008;377:679–90. https://doi.org/10.1016/j.jmb.2007.10.074.
16. Warbrick E. The puzzle of PCNA's many partners. BioEssays. 2000;22:997–1006. https://doi.org/10.1002/1521-1878(200011)22:11<997::AID-BIES6>3.0.CO;2-#.
17. Gomes XV, Burgers PMJ. Two modes of FEN1 binding to PCNA regulated by DNA. EMBO J. 2000;19:3811–21. https://doi.org/10.1093/emboj/19.14.3811.
18. Chapados BR, Hosfield DJ, Han S, Qiu J, Yelent B, Shen B, et al. Structural basis for FEN-1 substrate specificity and PCNA-mediated activation in DNA

replication and repair. Cell. 2004;116:39–50. https://doi.org/10.1016/S0092-8674(03)01036-5.
19. Sakurai S, Kitano K, Yamaguchi H, Hamada K, Okada K, Fukuda K, et al. Structural basis for recruitment of human flap endonuclease 1 to PCNA. EMBO J. 2005;24:683–93. https://doi.org/10.1038/sj.emboj.7600519.
20. Tsutakawa SE, Classen S, Chapados BR, Arvai AS, Finger LD, Guenther G, et al. Human flap endonuclease structures, DNA double-base flipping, and a unified Understanding of the FEN1 superfamily. Cell. 2011;145:198–211. https://doi.org/10.1016/j.cell.2011.03.004.
21. Tian Y, Li N, Li Q, Gao N. Structural insight into Okazaki fragment maturation mediated by PCNA-bound FEN1 and RNaseH2. EMBO J. 2024;44:484–504. https://doi.org/10.1038/s44318-024-00296-x.
22. Strzalka W, Oyama T, Tori K, Morikawa K. Crystal structures of the Arabidopsis thaliana proliferating cell nuclear antigen 1 and 2 proteins complexed with the human p21 C-terminal segment. Protein Sci. 2009;18:1072–80. https://doi.org/10.1002/pro.117.
23. Strzalka W, Kaczmarek A, Naganowska B, Ziemienowicz A. Identification and functional analysis of PCNA1 and PCNA-like1 genes of Phaseolus coccineus. J Exp Bot. 2010;61:873–88. https://doi.org/10.1093/jxb/erp354.
24. Mcwhirter C, Tonge M, Plant H, Hardern I, Nissink W, Durant ST. Development of a high-throughput fluorescence polarization DNA cleavage assay for the identification of FEN1 inhibitors. J Biomol Screen. 2013;18:567–75. https://doi.org/10.1177/1087057113476551.
25. Shriver Z, Capila I, Venkataraman G, Sasisekharan R. Heparin and Heparan sulfate: analyzing structure and microheterogeneity. Handb Exp Pharmacol. 2012;207:159–76. https://doi.org/10.1007/978-3-642-23056-1_8.
26. Lieber MR. The FEN-1 family of structure-specific nucleases in eukaryotic DNA replication, recombination and repair. BioEssays. 1997;19:233–40. https://doi.org/10.1002/bies.950190309.
27. Gloor JW, Balakrishnan L, Bambara RA. Flap endonuclease 1 mechanism analysis indicates flap base binding prior to Threading. J Biol Chem. 2010;285:34922–31. https://doi.org/10.1074/jbc.M110.165902.
28. Sobhy MA, Joudeh LI, Huang X, Takahashi M, Hamdan SM. Sequential and multistep substrate interrogation provides the scaffold for specificity in human flap endonuclease 1. Cell Rep. 2013;3:1785–94. https://doi.org/10.1016/j.celrep.2013.05.001.
29. Schrodinger L. The PyMOL Molecular Graphics System, Version 3.0 Schrödinger, LLC. 2024.

Publisher's note